Advances in Science and Technology Research Journal

Advances in Science and Technology Research Journal 2022, 16(5), 1–10
https://doi.org/10.12913/22998624/152821
ISSN 2299-8624, License CC-BY 4.0

Received: 2022.07.19
Accepted: 2022.10.17
Published: 2022.11.01

Suppressing of Co-Extracted Electrons in a Negative Ion Source – Numerical Simulations

Marcin Turek[1*], Paweł Węgierek[2]

[1] Institute of Physics, Maria Curie-Skłodowska University, pl. M. Curie-Skłodowskiej 1, 20-031 Lublin, Poland

[2] Faculty of Electrical Engineering and Computer Science, Lublin University of Technology ul. Nadbystrzycka 38 D, 20-618 Lublin, Poland

* Corresponding author's e-mail: mturek@kft.umcs.lublin.pl

ABSTRACT

Electron co-extraction and suppression by a transverse magnetic fields is studied within a two dimensional particle-in-cell numerical model of surface ionisation ion source with beveled extraction opening. A novel approach of data presentation is proposed, based on the fact that dependences of co-extracted current on the filter strength could be approximated by four parameters only, describing e.g. initial electron current value and cut-off B value. In the paper the influence of extraction system geometry is considered – it is shown that the cut-off B value increases with the size of the opening in the extraction electrode, while the inclination of the extraction opening walls does not play any significant role. It is demostrated that the most of electron is eliminated by hiting the extraction electrode walls, however up to 30% of electrons were lost by encountering the extraction channel walls due to the modification of their trajectories by the filter field. The influence of the magnetic filter field placement is also investigated – the center of the filter field has to be no further than 2 mm form the extraction channel orifice in order to achieve minimal values of the cut-off field (~20 mT). The possibly low extraction voltages are preferable, as the ammount of co-extracted electrons grows rapidly with V_{ext} resulting in e.g. threefold increase of cut-off parameter value when extraction voltage is changed from 1 kV up to 10 kV. Within the considered model the filter field does not have any significant influecne on extracted H^- current.

Keywords: Particle-in-cell simulations, negative ion sources, ion beam extraction.

INTRODUCTION

Negative ion sources of various kinds are used in numerous fields of research, including mass spectroscopy and nuclear and particle physics (tandem accelerators, cyclotrons). However, the most prominent example of their usefulness are neutral beam injections systems of nuclear fusion devices [1, 2], where large volume high power negative ion sources are employed to produce high power neutral particle beams being insensitive to magnetic field and allow heating Tokamak plasma without inducing different kinds of instabilities. NBI systems of the ITER reactor are designed to provide 33 MW of power using 1 MeV neutral deuterium/hydrogen beams [3, 4]. In order to achieve such performance, large area (0.9×1.9 m) low pressure (~0.3 Pa, in order to minimize stripping losses of negative ions) RF-inductively coupled ion sources providing current densities of ~30 mA/cm^2 are required [5–8]. In such sources negative ion sources are produced mostly in surface conversion process [9] on caesium covered first grid (plasma grid) of the extraction system. The surface ionisation mechanism after a proper conditioning of the ion source is known to prevail over the volume production [9, 10].

Extraction of negative ion beams, especially those of large intensity, implies a burning issue of co-extracted electrons [3, 11, 12]. Massive electron co-extraction of electrons results in a very large space-charge that could hinder negative ion extraction and also spoils the acceleration system

efficiency [2]. This problem is usually solved by removing electrons due to application of special magnetic filters in the region of ion source opening and the extraction system. Another counter measure is applying a positive bias to the plasma grid in order to make it electron-attracting and suppress the unwanted electron current [13].

Numerical modeling of ionization and ion beam formation and extraction for decades supports design of ion sources and helps understanding of processes occurring within them. Over last years a plethora of numerical models of negative ion beam production were presented in literature [14–22].

In the paper a 2D numerical model of surface H- production and beam formation, initially presented in [23,24] and then upgraded to take account ionization on beveled extraction channel surfaces [25] and to calculate ion beam emittance [26], is used to study the influence of transverse magnetic field filter having gaussian profile on electron co-extraction. Using lower dimension model is commonly accepted technique [27, 28] that allows reduce computational effort and, if performed carefully, still allows obtaining meaningful and valuable results. Despite lowered dimensionality, the applied model seems much more reliable than that presented in [29,30] as this time the cell sizes are much shorter than plasma Dirac length. One should have in mind that the presented code could be run on a single CPU workstation and the typical computation time is of order of one day, while a typical 3D code requires hundreds of CPUs of a supercomputer or a Linux class cluster. The model describes creation of negative ions not only at caesiated (i.e. with lowered work function [31]) surface plasma grid facing the ion source chamber but also at the chamfered (inclined) surfaces of the extraction channel. Besides the brief description of the numerical models some results of the influence of the magnetic filter in different configuration of the extraction system is presented. Based on the fact that the dependence of the extracted electron current on the magnetic filter strength look similar independently on which aspect of the extraction system is studied, a novel approach enabling optimisation of the system is proposed. As each of $I_{electr}(B)$ curves could be approximated by 4 parameters (two electron current values and two magnetic field cut-off values) it is justified to follow the evolution of these parameters with e.g. extraction voltage or electrode opening size, which makes the data presentation and discussion more effective. The papers presents results of electron co-extraction and suppression which may be affected by factors like the geometry of the extraction channel (its size and inclination of the walls), the diameter of the opening in the extraction electrode as well as the position of the magnetic filter. The role played by the extraction voltage is also under investigation.

SIMULATION MODEL

The model used for simulations is based on the PIC (Particle-In-Cell) method [32]. Within that approach each computational particle represents a large number of real particles moving the same way what enables large reduction of the numerical effort. Some limitations should be however kept in mind: (1) each mesh cell should contain sufficient number of computational particles (30–50 is a rule-of-a-thumb). (2) the cell size should be smaller than the plasma Debye length, (3) the simulation timestep Δt should be chosen so that the Courant–Friedrichs–Lewy criterion [33] is fulfilled:

$$v\Delta t / \Delta x < 1 \tag{1}$$

where: v – maximal particle velocity in the plasma. The timestep should be also smaller than the inverse of the plasma frequency. In the paper a 2D model of a small ionization chamber of length L = 4.5 mm and width 5 mm.

The sketch of the simulated system is shown in Figure 1. A flat extraction electrode on the negative extraction potential V_{ext} is placed at the distance d from the extraction hole. The radius of the opening in the extraction electrode is marked as r_e. As in previous papers [23,24], both negative ions and electrons are extracted from the chamber through a conical channel. Its geometry is described by the channel length h and its inner and outer radii r_i and $r_{o,}$ respectively. The area of simulation is covered by a rectangular 160×100 grid with cell sizes $\Delta x = \Delta y$ = 0.05 mm. The ionization chamber is initially filled with 10^7 macroparticles representing either electrons or H^+ ions (both species are represented by equal numbers of computational particles). The first step of the PIC procedure is the determination of charge

density distribution by assigning computational particle charges to grid points. Having this done, the electrostatic potential distribution could be found by solving the Poisson equation:

$$\Delta V(x,y) = -\frac{\rho(x,y)}{\varepsilon_o} \tag{2}$$

where: with additional boundary conditions being the result of the presence of electrodes. This is achieved using successive over-relaxation method (SOR) as described in the case of 2D [23,24] and 3D [29, 30] Particle in-Cell codes. Once the potential and charge distributions are derived, the electric field in the grid points is calculated by numerical integration.

As it was already mentioned a transverse (in the *z* direction) magnetic filter field was placed in the extraction region in order to get rid of electrons from the extracted beam. The applied filter profile was gaussian:

$$B(x) = B_o \exp\left[\frac{(x-x_o)^2}{2w^2}\right] \tag{3}$$

where: x_o = 3 mm,
w = 2 mm, unless otherwise stated. The strength of the magnetic filter changed up to 40 mT. Such a profile is shown in the upper part of the Figure 1.

As the magnetic field affects trajectories of charged particles according to Lorentz equations

$$m\ddot{\vec{r}}(t) = q\left(\vec{E}(\vec{r},t) + \dot{\vec{r}} \times \vec{B}(\vec{r})\right) \tag{4}$$

where: q and m – particle charge and mass, the velocity Verlet particle pusher algorithm was modified as in [34] (see equations 4 and 5 therein). An additional care has to be taken in order to make sure that the simulation timestep is smaller than the inverse of the electron Larmor frequency:

$$\Omega = \frac{eB}{m_e} \tag{5}$$

where: e and m_e – the electron charge and mass, respectively. As the new particle positions and velocities are found, it is possible to determine the new charge density distribution and the whole simulation loop is repeated as long as necessary.

Negative hydrogen ions start to be injected into the chamber as soon as a quasi-stationary state is achieved with balanced plasma (which takes usually 2×10^4–3×10^4 timesteps). The injection rate is kept constant (N_{H^-} per Δt), this rate is related to neutral-negative ion conversion that takes place at caesium-covered inner surfaces of plasma grids in negative ion sources. H^- ions are ejected not only from inner surface of the plasma grid of the chamber (as in [27, 28]) but also from the inner (chamfered) walls of the extraction channel, as in the previous paper [23]. Initial velocities of negative H ions correspond to kT = 0.25 eV and they undergo numerous elastic collisions with other charged particles, which is simulated using Monte Carlo BCA (binary collision approximation) [23,35]. The extracted electron and ion current are registered at the planes marked by dashed lines in Figure 1: s_1 (outer rim of the extraction channel x = 5.5 mm) and s_2 (entrance of the opening in the extraction electrode, x = 7.5 mm). The numerical program is able to register e.g. evolution of potential values in selected points of the chamber, total numbers number of particles inside the chamber and also charge density as well as electrostatic potential distributions snapshots.

SIMULATION RESULTS

A the first stage the numerical simulations for B_o changing up to 40 mT were performed in order to check the influence of the magnetic filter field on the extraction of negative particles (mainly electrons) for different geometries of the extraction channel. This geometry is described by r_o = 0.7 mm while r_i changes from 0.8 mm up to 2 mm. As the length of the extraction channel is kept constant (equal to 1 mm) the inclination of extraction opening walls changes in a broad range. Calculations were performed for V_{ext} = 1 kV, d = 2 mm and 160000 time steps (with Δt=0.2×10^{-11} s). The radius of the opening on the flat extraction electrode was r_e = 1.2 mm. Charge density of plasma was set to 10^{16} m^{-3} and its electron temperature to kT = 1 eV. The negative ion injection rate was N_{H^-} = 300.

As one can see in Figure 2. the magnetic field does not influence the extracted negative

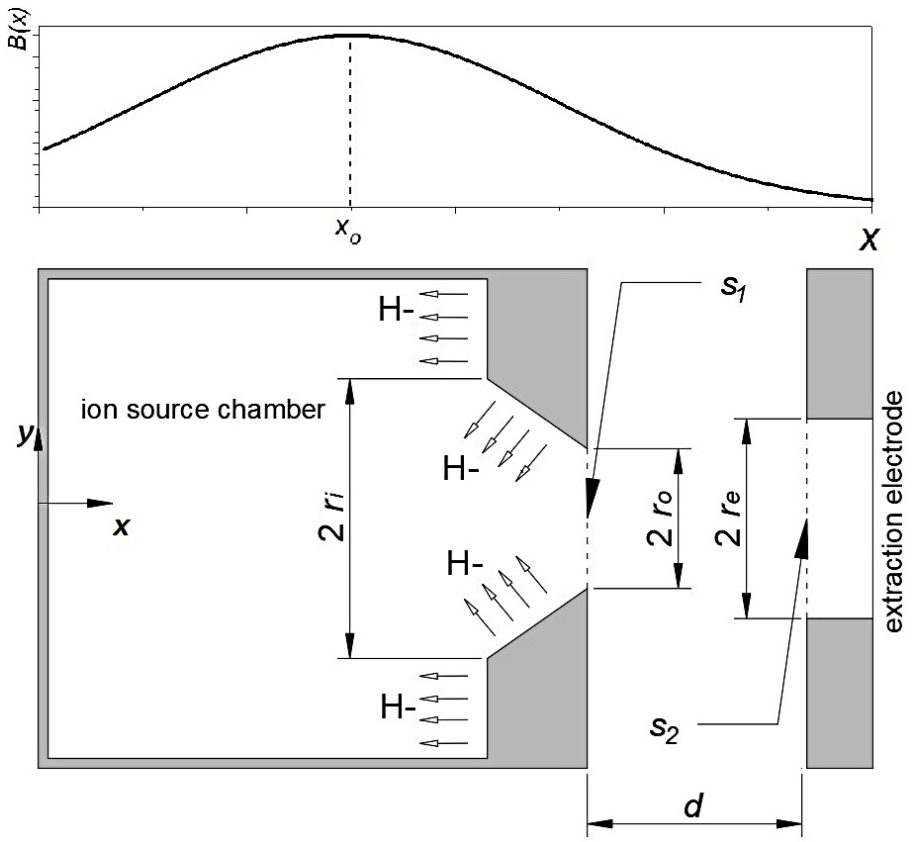

Fig. 1. Schematic view of the simulated system. An example of the magnetic filter field is shown in the upper part of the picture

ion current. This differs from results obtained using both 2D [10] and 3D [15, 18, 29]. That difference is probably due to the fact that most of the negative ions are produced very near to the extraction channel (especially in the case of large r_i values) and they are immediately caught by the accelerating field, while in the case of above mentioned codes one deals with the flux of negative ions produced in the volume process. Moreover, the model does not takes losses due to electron stripping in ion-electron collisions in the extraction region. As it was previously shown, the extracted H^- current strongly depends on the extraction channel wall inclination [24]. This is also true in the considered case – the H^- current is almost by 4 times larger when the r_o = 2 mm, compared to the nearly cylindrical extraction channel.

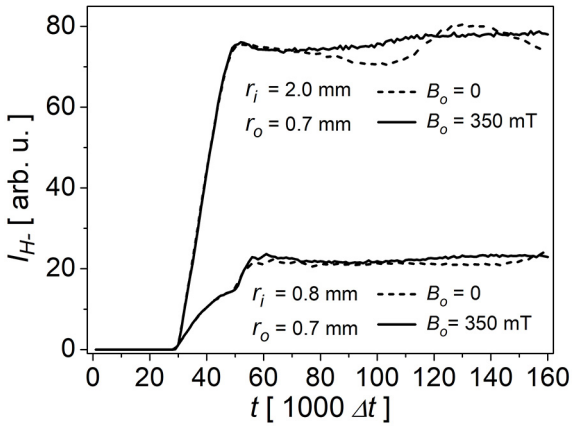

Fig. 2. Dependences of the extracted H- current (IH-) on simulation time t (a simulation timestep Δt is the unit of time). Results obtained for the two shapes of the extraction channel. Calculations done with and without the magnetic filter

On the other hand the extracted electron current changes dramatically with the strength of the magnetic filter. As one can see in Figure 3 the current measured at the extraction electrode entrance (plane s_2), which is initially by an order of magnitude larger than I_{H-} decreases with B_o and almost vanishes for B_o = 30 mT. This is in a good qualitative agreement with results presented e.g. in [36], one should have in mind that a different geometry of extraction system is considered therein. Moreover one can see current oscillations with the period of ~50000 Δt, their amplitude decreases with B_o. The filtering mechanism is quite easy to understand when one looks at Figure 4. (right part).

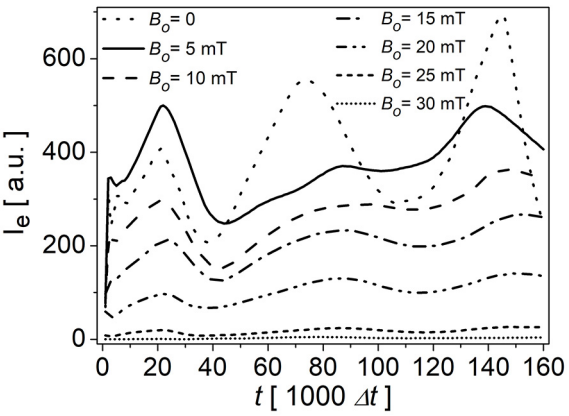

Fig. 3. Evolution of the co-extracted electron current Ie for different values of B_o. Results for Uext = 1 kV, r_o = 0.7 mm, r_i = 1.5 mm and r_e = 1.2 mm. As in Fig. 2 the timestep Δt is the unit of simulation time t

The electron beam enters completely the opening of the extraction electrode (having radius r_e = 1.2 mm), despite the fact that the beam is divergent. As the strength of the magnetic filter increases the electron trajectories are more and more deflected. Similar electron trajectory bending was observed e.g. in the case of ONIX simulations [15]. As one can see in the case of B_o=10 mT, part of the beam passes the entrance while the other part of the beam is stopped at the electrode. For even stronger filter fields (as in the presented case B_o = 35 mT) the electron beam is bent and most of particles hits the electrode – the current measured at s_2 nearly vanishes. It should be also noticed that the filter field changes the electron distribution inside the chamber. Looking at the H^+ distributions, which have to adjust to

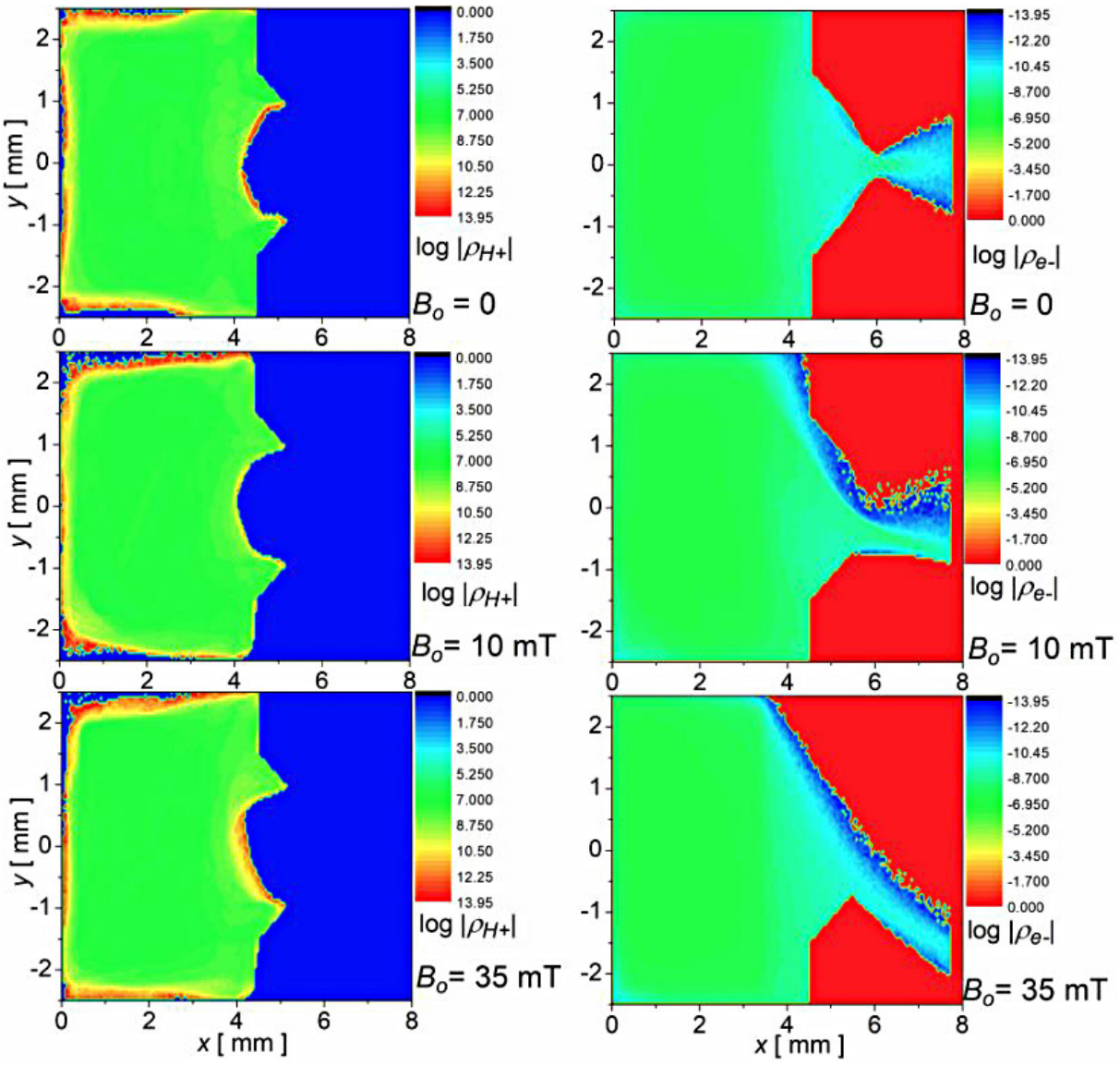

Fig. 4. Examples of the H^+ and e- charge density distributions in x and y coordinates (see Fig. 1 for explanation) at the final stage of simulations for different values of the filter field. Simulations done for U_{ext} = 1 kV

electron and H^- distribution in order to maintain plasma neutrality, one can see that the shape of the plasma meniscus near the extraction opening also becomes strongly asymmetric. Such formation of asymmetric meniscus was shown in [18, 36]

As in the following parts of the paper the influence of other parameters of the extraction system on electron filtering will be presented, some much more synthetic way of data presentation is proposed. Instead of showing a family of current(time) curves obtained for different values of the filtering field B_o the average values of electron current for each curve as the function of B_o could be presented, as shown in Figure 5.

It should be noted that *current*(*filter field*) characteristics both for s_1 (extraction opening) and s_2 (extraction electrode) could be easily shown and compared. Both $I_1(B_o)$ and $I_2(B_o)$ curves could be approximated with three straight line segments: (1) for relatively small B_o the electron current is almost constant as the electrons pass the extraction opening undisturbed, at level I_A then (2) for intermediate B_o values almost linear decrease of the current is observed. This is due to the fact that increasing part of deflected electrons hits either the extraction channel walls in the plasma (first) electrode, either the front of the extraction (the second one) electrode. The last (3) segment of $I_1(B_o)$ correspond to the situation when the further increase of filter field (above ~B_B) does not changes the number of electrons passing the extraction opening – electrons coming from the upper part of the chamber (y>0) are still able to pass through the opening – an this current (I_B) is limited by charge density and extraction voltage. The interpretation of the last segment of $I_2(B_o)$ curve is rather trivial – all electrons are lost at the extraction electrode. The B_c could be considered as the cut-off value of the filter field – high enough to get rid of virtually all electrons. The characteristics presented in [36] correspond rather to $I_2(B_o)$ curves, but are presented as semi-log figure.

The shape of $I(B_o)$ curves is quite universal, however, changing the parameters of the extraction system (like the geometry of electrodes, extraction voltage, position of the filter field etc.) leads to the change of $I(B_o)$ curve parameters like I_A, I_B, B_B and B_C. One may think of taking one step further and presenting this set of parameters as a function of the chosen extraction system magnitude instead of a family (or rather two families) of $I(B_o)$ characteristics.

The first factor which influence is analyzed using the proposed approach is the entrance radius of the extraction channel r_i. The value of that radius changes from 0.8 mm (almost cylindrical extraction channel) up to 2 mm (large inclination of the extraction channel walls which makes the surface production very intense near the extraction opening). The calculations were made for x_o = 3 mm and w = 2 mm for the same value of extraction voltage V_{ext} = 1 kV. Consequently, one

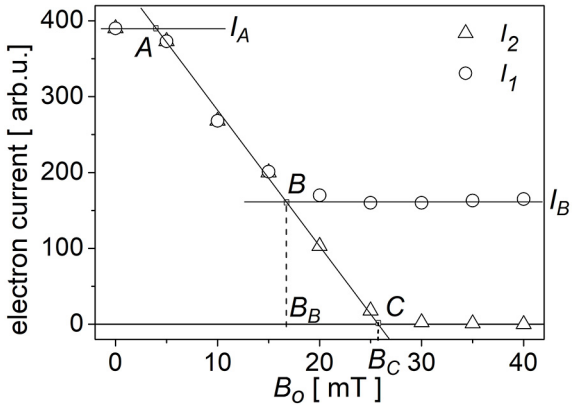

Fig. 5. Dependences of extracted electron currents (measured at the extraction opening I_1 and at the extraction electrode opening I_2) on the magnetic filter field strength Bo. The four parameters (I_A, I_B, B_B and B_C) that approximate $I_1(B_o)$ and $I_2(B_o)$ shape are introduced

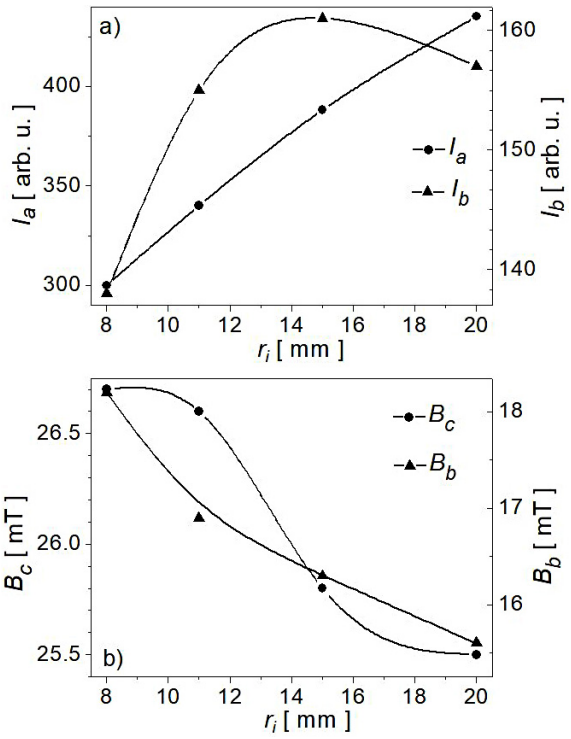

Fig. 6. Evolution of I_A, I_B (a) and B_B, B_C (b) parameters with the entrance radius r_i of the extraction channel

can see in Figure 6a that the initial I_a current increases nearly linearly with the radius r_i due to the more effective electron pulling through more and more wide extraction opening. However, the behavior of the saturated current passing the exit of the extraction channel (I_B) is more complex: one can see the wide maximum near r_i= 1.5 mm. The value of the cut-off filter field decreases with the inclination of the extraction channel walls but this effect is rather small (of order 1 of mT in the considered case). The trend of $B_B(r_i)$ is almost the same, as could seen in Figure 6b.

The influence of the size of the opening in the extraction electrode on filtering of co-extracted electrons is presented in Figure 7. The filter field is the same as in the previous case (x_o = 3 mm and w = 2 mm), while changes in the range from r_e = 0.8 mm up to r_e = 1.4 mm. As one may expect, the size of the opening in the second electrode has little to do with co-extracted currents measured at the first electrode – the values of I_A and I_B are nearly constant (Fig 7a). On the other hand, the changes of filter field intensity parameters are large (the required cut-off value, B_C increases almost twice with r_e rising in the considered range) and rather easy to understand. The larger is the size of the opening in the extraction electrode, the stronger magnetic filter is needed to drive the co-extracted electron beam off and make them hit the electrode surface. Hence, one may say that the systems with tighter opening in the extraction electrodes are preferred as far as avoiding negative ion beam contamination by electrons is considered.

As one may expect, not only the geometry of the extraction systems determines the intensity of extracted electrons. The placement of the filter field seems to be one of the most important parameters. Results of simulations for the different values of the filter field centroid x_o are gathered together in Figure 8. As in the previous case, the initial (B_o = 0) electron current does not change with x_o. However, the saturation current I_B decreases fourfold as the filter moves from x_o = 1 mm to x_o = 5 mm (at the s_1 plane). The strong magnetic field in the extraction channel is able to deflect electrons trying to pass it and make them hit their inner walls. Putting the filter field deep into the plasma region results in extremely high cut-off values (~150 mT for x_o = 1). The values of B_C decrease very fast to approximately 25 mT as x_o is 4 mm (filter in the extraction channel region). The B_B values evolve in a similar way, but the saturation of the extracted electron current takes place for much smaller B_o values than the cut-off value (in the range from 150 mT up to 60 mT).

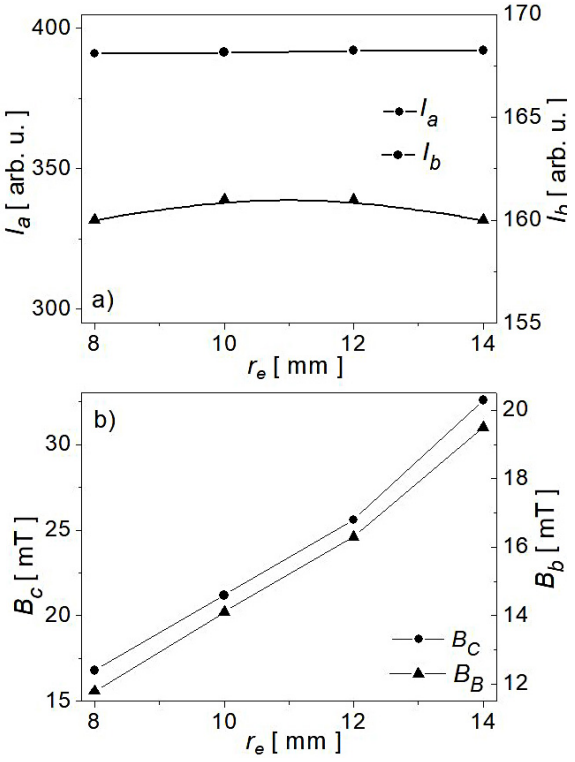

Fig. 7. Evolution of I_A, I_B (a) and B_B, B_C (b) values with the radius re in the extraction electrode

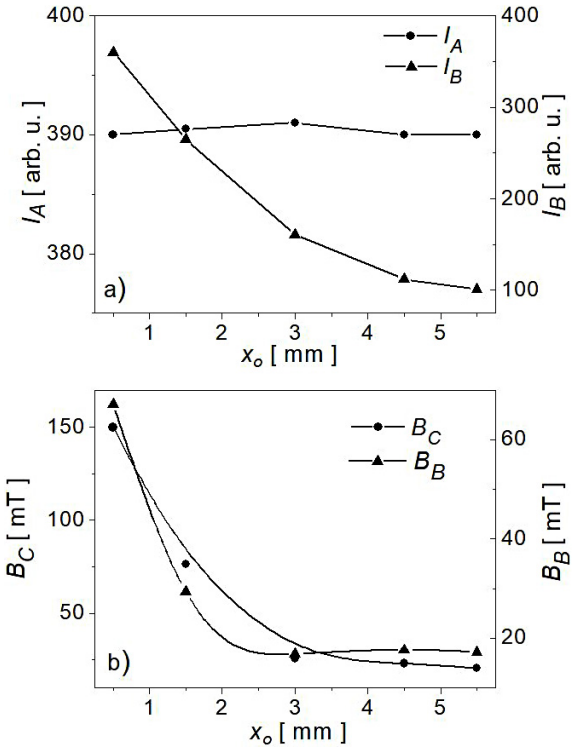

Fig. 8. Dependence of I_A, I_B (a) and B_B, B_C (b) values on the center position xo of the magnetic filter field

The value of the extraction voltage is the next factor influencing the co-extraction and filtering of electron from the ionization chamber. The simulations were performed for r_i = 1.5 mm, r_o = 0.7 mm and r_e = 1.2 mm, the plasma parameters were kept as in the previously considered cases. The number of electrons being pulled out by a positive biasing of the extraction electrode strongly depends on the bias. The $I_A(V_{ext})$ dependency (current-voltage curve) is almost perfectly straight line in the considered voltage range (up to 10 kV). This could be understood in the light of high electron mobility and concentration in the extraction region – in matter of fact current-voltage curves for H^- ions (much slower than electrons) in that voltage range are also far from the saturation region. The current voltage curve measured at the extraction electrode $I_B(V_{ext})$ has slightly different shape, as the rising extraction voltage influences strongly on the shape of the electron beam, making it harder to deflect. This effect is especially well visible also for $B_B(V_{ext})$ and $B_C(V_{ext})$. The filter field cut-off value increases almost 3 times as the extraction voltage grows from 1 kV up to 10 kV. Figure 9 shows influence of the extraction voltage U_{ext} on I_A, I_B (a) and B_B, B_C (b) parameters describing the electron extraction.

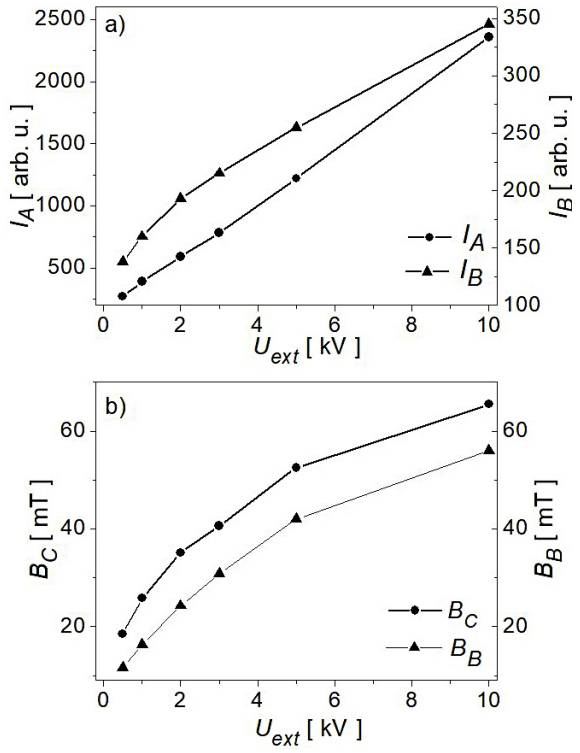

Fig. 9. Influence of the extraction voltage U_{ext} on I_A, I_B (a) and B_B, B_C (b) parameters describing the electron extraction

CONCLUSIONS

The influence of magnetic filter field placed in the extraction region on the electron extraction is studied using a 2D particle-in-cell model. An extensive study of electron current dependences on filter field $I(B_o)$ for different parameters characterizing the extraction system was demonstrated. An universal pattern of $I(B_o)$ curves is found. The above-mentioned universality enabled reduction of the presented data to four parameters (I_A, I_B, B_B and B_C), carrying most of the information on $I(B_o)$ behavior. Within the considered model the magnetic filter does not influence extracted H^- current, while the co-extracted electron current is suppressed due to trajectory deflection. For most of the considered configurations even very strong filter fields (several tens of mT) result in I_B values being ~30 % of I_A. It was shown that cut-off values of the magnetic filter do not depend much on the inclination of the extraction channel walls. On the other hand, it was demonstrated that cut-off values increase strongly with the size of the opening in the extraction electrode – systems with small extraction openings enable easier electron filtering. The B field cut-off values reach minimal values (~ 20 mT) when the filter is placed very near to the extraction region. The $I_A(U_{ext})$ and $I_B(U_{ext})$ i.e current-voltage curves are almost straight lines in the considered voltage region (up to 10 kV). The required filter field parameters increases nearly three times when U_{ext} is changed from 1 kV up to 10 kV.

Acknowledgements

The publication of the paper is supported by the "Excellence in Science" program of the Polish Ministry of Education and Science (*International Conference "Ion Implantation and Other Applications of Ions and Electrons ION2020"*)

REFERENCES

1. Inoue T., Pietro E. D., Hanada M., Hemsworth R. S., Krylov A., Kulygin V., Massmann P., Mondino P.L., Okumura Y., Panasenkov A., Speth E., and Watanabe K., Design of neutral beam system for ITER-FEAT, Fusion Eng. Design 2001; 56–57: 517–521.
2. Hemsworth R.S., Inoue T. Positive and negative ion sources for magnetic fusion, IEEE Trans. Plasma Sci. 2005; 33(6): 1799–1813.

3. Hemsworth R., Tanga A., Antoni V. Status of the ITER neutral beam injection system (invited), Rev. Sci. Instrum. 2008; 79(2): 02C109.
4. Hemsworth R. et al. Status of the ITER heating neutral beam system, Nucl. Fusion. 2009; 49(4): 045006.
5. Speth E., Falter H. D., Franzen P., Fantz U. et al. Overview of the RF source development programme at IPP Garching, Nucl. Fusion. 2006; 46(6): S220.
6. Kraus W., Fantz U., Franzen P., Fröschle M., Heinemann B., Riedl R., Wünderlich D. Rev Sci Instrum. The development of the radio frequency driven negative ion source for neutral beam injectors (invited), Rev. Sci, Instr. 2012; 83(2): 02B104.
7. Sonato P., Agostinetti P., Anaclerio G., Antoni V., Barana O., Bigi M., Boldrin M., Cavenago M., Dal Bello S., Dalla Palma M. et al., The ITER full size plasma source device design, Fusion Eng. Des. 2009; 84(2–6): 269–274.
8. Toigo V., Piovan R., Bello S. D., Gaio E., Luchetta A., Pasqualotto R., Zaccaria P., Bigi M., Chitarin G., Marcuzzi D. et al. The PRIMA Test Facility: SPIDER and MITICA test-beds for ITER neutral beam injectors, New J. Phys. 2017; 19: 085004.
9. Wunderlich D., Schiesko L., McNeely P., Fantz U., Franzen P., and NNBI- ¨ Team, On the proton flux toward the plasma grid in a RF-driven negative hydrogen ion source for ITER NBI, Plasma Phys. Controlled Fusion. 2012; 54(12): 125002.
10. Bacal M., Wada M. Negative hydrogen ion production mechanisms, Appl. Phys. Rev. 2015; 2(2): 021305.
11. Fantz U., Franzen P., Kraus W., Berger M., Christ-Koch S., Falter H., Froschle M., Gutser R. et al. Physical performance analysis and progress of the development of the negative ion RF source for the ITER NBI system, Nucl. Fusion. 2009; 49(12): 125007.
12. Rafalskyi D., Aanesland A. Electron-less negative ion extraction from ion-ion plasmas, Appl. Phys. Lett. 2015; 106(10): 104101.
13. Wimmer C., Fantz U. NNBI-Team. Extraction of negative charges from an ion source: Transition from an electron repelling to an electron attracting plasma close to the extraction surface, J. Appl. Phys. 2016; 120(7): 073301.
14. Mochalskyy S., Lifschitz A.F. and Minea T. Extracted current saturation in negative ion sources, J. Appl. Phys. 2012; 111(11): 113303.
15. Mochalskyy S., Wuenderlich D., Fantz U., Towards a realistic 3D simulation of the extraction region in ITER NBI relevant ion source, Nuclear Fusion. 2015; 55(3): 033011.
16. Fubiani G., Boeuf J.P. Three-dimensional modeling of a negative ion source with a magnetic filter: impact of biasing the plasma electrode on the plasma asymmetry, Plasma Sources Science & Technology. 2015; 24(5): 055001.
17. Nishioka S., Goto I., Miyamoto K., Hatayama A., Fukano A., Study of ion-ion plasma formation in negative ion sources by a three-dimensional in real space and three-dimensional in velocity space particle in cell model, J. Appl. Phys. 2016; 119(2): 023302.
18. Fubiani G., Garrigues L., Hagelaar G., Kohen N. and Boeuf J. P., Modeling of plasma transport and negative ion extraction in a magnetized radio-frequency plasma source. New J. of Phys. 2017; 19(1): 015002.
19. Garrigues L., Fubiani G., Boeuf J.P. Negative ion extraction via particle simulation for fusion: critical assessment of recent contributions, Nucl. Fusion. 2017; 57(1), 014003.
20. Shah M., Chaudhury B., Bandyopadhyay M., Chakraborty A. Computational characteristics of plasma transport across magnetic filter in ROBIN using PIC-MCC simulation, Fusion Eng. Des. 2020; 151: 111402.
21. Kanki T., Himura H., Tsumori K., Nakano H. Simulations of negative ion extraction and transport for developing novel remote reactive ion processing system, Jpn. J. Appl. Phys. 2020; 59(SJ): SJJE01.
22. Demerdjiev A., Goutev N., Tonev D. Simulations of negative hydrogen ion sources. J. Phys.: Conf. Ser. 2018; 1023: 012033.
23. Turek M., Węgierek P. Negative Ion Beam Emittance Calculations, Devices and Methods of Measurements. 2020; 11(1): 42–52.
24. Turek M. Negative Ion Beam Production in an Ion Source with Chamfered Extraction Opening, Acta Physica Polonica A. 2019; 136(2): 322–328.
25. Turek M. Two-Dimensional Simulations of H-Ions Extraction, Acta Physica Polonica A. 2017; 132(2); 254–258.
26. Turek M. Symulacje PIC plazmy w źródle jonów ujemnychPrzeglad Elektrotechniczny. 2016; 92(8): 162–165.
27. Wunderlich D., Gutser R., Fantz U. PIC code for the plasma sheath in large caesiated RF sources for negative hydrogen ions, Plasma Sources Sci. Technol. 2009; 18(4): 045031.
28. Boeuf J.P., Claustre J., Chaudhury B., Fubiani G. Physics of a magnetic filter for negative ion sources. II. E × B drift through the filter in a real geometry, Phys. Plasmas. 2012; 19(11): 113510.
29. Turek M., Sielanko J. Simulations of negative ion extraction from a multi-aperture ion source in the presence of the magnetic filter, Vacuum. 2009; 83(S1): 256–261.

30. Turek M., Sielanko J., Franzen P., Speth E. Influence of transversal magnetic field on negative ion extraction process in 3D computer simulation of the multi-aperture ion source AIP Conf. Proc. 2006; 812(1): 153.
31. Fantz U., Franzen P., Kraus W., Berger M., Christ-Koch S., Fröschle M., R. Gutser, Heinemann B., Martens C., McNeely P., Riedl R., Speth E., Wünderlich D. Negative ion RF sources for ITER NBI: status of the development and recent achievements, Plasma Phys. Control. Fusion. 2007; 49(12B): B563.
32. Birdsall C.K., Langdon A.B. Plasma Physics Via Computer Simulation, McGraw-Hill, 1985.
33. Courant R., Friedrichs K.O., Levy H. Über die partiellen Differenzengleichungen der mathematischen Physik, Math. Ann. 1928; 100(1): 32–47.
34. della Valle E., Marracino P., Setti S., Cadossi R., Liberti M. and Apollonio F., Magnetic molecular dynamics simulations with Velocity Verlet algorithm, 2017 XXXIInd General Assembly and Scientific Symposium of the International Union of Radio Science (URSI GASS), Montreal, QC 2017; 1–4. DOI: 10.23919/URSIGASS.2017.8105168
35. Ma S., Sydora R.D., Dawson J.M. Binary collision model in gyrokinetic simulation plasmas, Comp. Phys. Comm. 1993; 77(2): 190–206.
36. Boeuf J.P., Chaudhury B., Garrigues L. Physics of a magnetic filter for negative ion sources. I. Collisional transport across the filter in an ideal, 1D filter Physics of Plasmas. 2012; 19(11): 113509.